Journal of Physiology (1991), **437**, *pp.* 221–238
With 9 figures
Printed in Great Britain

ACTIVATION KINETICS OF CALCIUM CURRENTS IN BULL-FROG SYMPATHETIC NEURONES

BY FRANCISCO SALA

From the Howard Hughes Medical Institute, Department of Neurobiology and Behavior, State University of New York, Stony Brook, NY 11794-5230, USA

(*Received 28 August 1990*)

SUMMARY

1. Calcium currents were recorded in dissociated bull-frog sympathetic neurones (BSNs) through patch pipettes using discontinuous voltage clamp. Activation kinetics were examined by analysing turn-on and turn-off currents.

2. After short depolarizing pulses turn-off tail currents were fitted with the sum of two exponentials. The fast component (time constant, $\tau \approx 240$ μs at -40 mV) was undoubtedly due to the closure of calcium channels. The significance of a small and slower component is discussed.

3. Neither activation nor deactivation time courses changed as channels inactivated during progressively longer pulses or when the holding potential was less negative. No specific component was selectively suppressed by these manipulations.

4. Steady-state activation of the Ca^{2+} current was described by the Boltzmann distribution raised to the second power. Currents had an apparent threshold at -30 mV and were half-activated at $+5$ mV.

5. Calcium current turned on following m^2 kinetics throughout the range of activation. The slowest time constant was around 1·2 ms between 0 and $+10$ mV. Turn-on was faster at negative or more positive potentials.

6. The time course of decay of tail currents became progressively faster at more negative potentials.

7. The instantaneous current–voltages (I–V) curve was obtained from tail current measurements and fitted by a modified constant-field equation.

8. The measured peak I–V curve could be reconstructed from the activation curve and the instantaneous I–V curve.

9. The activation kinetics of the calcium current in BSNs were consistent with the existence of a single kinetic class of channels and can be described with a simple m^2 Hodgkin–Huxley model.

INTRODUCTION

Calcium current activation kinetics in nerve cells have been difficult to analyse due to their fast time course. Their study requires both proper spatial and temporal voltage-clamp conditions which are not always achieved by conventional techniques.

* Permanent address: Departamento de Neuroquímica., Facultad de Medicina, Universidad de Alicante, 03080 Alicante, Spain.

MS 8754

In this report, discontinuous single-electrode voltage-clamp switching at high frequencies was used in bull-frog sympathetic neurones (BSNs) to measure fast tail currents and turn-on currents corresponding to the closure and opening of calcium channels, respectively. Such a fast voltage clamp is achieved by using low-resistance patch pipettes in the whole-cell configuration (Jones, 1987). An accurate description of calcium current activation kinetics is important for understanding the roles of intracellular calcium in these cells, such as activation of potassium currents.

Since calcium currents carried through different types of channels have been described in this and other preparations (Tsien, Lipscombe, Madison, Bley & Fox, 1988), the first question is how many components could be resolved by tail current analysis. Such a procedure has proved to be helpful in distinguishing different types of channels (Matteson & Armstrong, 1986). Various protocols that according to Nowicky, Fox & Tsien (1985) should dissect tail current components were tested but no evidence for such different components was found. Regardless of the possible existence of two or more types of calcium channels whose currents could be separated by other means, it is concluded that calcium currents in BSNs can be treated as flowing through a kinetically homogeneous population of channels insofar as macroscopic activation and deactivation are concerned.

Recently, a report appeared describing calcium currents in BSNs with m^1 Hodgkin–Huxley kinetics (Jones & Marks, 1989). The same scheme was adopted previously after using two-microelectrode voltage clamp (Adams, 1980). In contrast, the present study has found the kinetics to be faster and better described by the m^2 Hodgkin–Huxley model.

Part of this work has been published in short form (Sala & Adams, 1989).

METHODS

Cell preparation and solutions

Isolated neurones were obtained from dissociated paravertebral sympathetic ganglia of adult bull-frogs (*Rana catesbeiana*) and kept in culture media at 4 °C for 0–7 days as described previously (Kuffler & Sejnowski, 1983). Cells lacking processes and with diameters of 40–60 μm (which presumably correspond to B-type cells) were used. All experiments were done at room temperature (20–22 °C).

The composition of the solutions used was chosen in order to minimize contaminating currents. Recording external solution contained (in mM): 20 TEACl; 5 4-aminopyridine (4-AP); 2 CsCl; 4 $CaCl_2$; 190 sucrose; 5 Tris; pH was adjusted to 7·2 with HCl. Soft glass patch-clamp electrodes were filled with (mM): 100 CsCl; 20 TEACl; 5 MgATP; 5 HEPES; 5 BAPTA; pH 7·2 adjusted by adding CsOH. Electrode resistances ranged from 0·5 to 1·5 MΩ when filled with internal solution.

Offset potentials

The liquid junction potential between the external and internal solutions was directly measured and found to be around 4 mV, the potential inside the electrode being negative. Furthermore, all voltage-dependent parameters slightly shifted to more negative values during the course of the experiments. This usually has been attributed to the dissipation of a Donnan potential during dialysis of the cell interior through the pipette (Marty & Neher, 1983). In some cells that lasted enough to stabilize (> 1 h), the measured shift was between 5 and 10 mV. Provided that all the experiments were done within 10–20 min after rupturing the patch, and for the sake of simplicity, it was assumed that the actual membrane potential was always 10 mV more negative than the observed values. All figures and text show the corrected values.

Voltage clamp

An Axoclamp-2A amplifier (Axon Instruments, Burlingame, CA, USA) was used to obtain whole-cell recordings (Hamill, Marty, Neher, Sakmann & Sigworth, 1981). Cells were clamped using the discontinuous single-electrode voltage-clamp mode (dSEVC), switching at 42–50 kHz with a

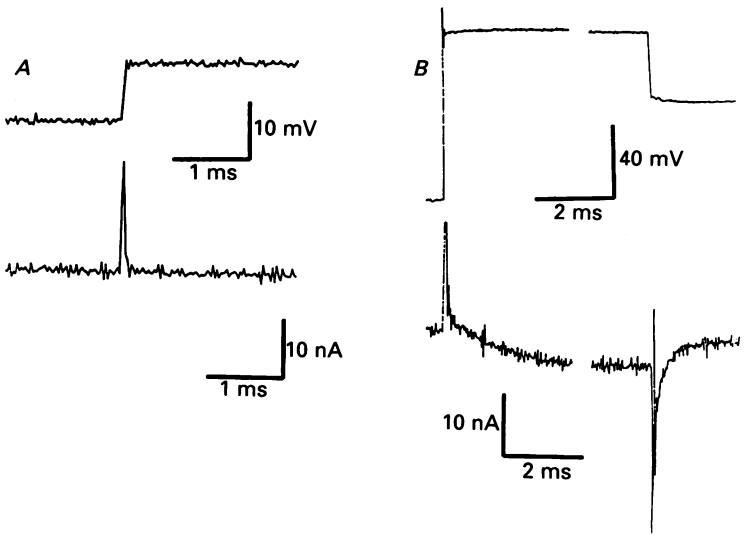

Fig. 1. Voltage-clamp performance. *A*, voltage and current traces for a subthreshold depolarizing pulse. Cell capacitance determined from the area under the capacitive transient was 67·5 pF (cell diameter was 45 μm). Average cell capacitance was 78·7 $\pm$ 26·0 pF ($n = 25$). Specific membrane capacitance was 1·04 $\pm$ 0·17 μF/cm^2, calculated from the observed cell diameters (48·9 $\pm$ 7·1 μm). Numbers are means and standard deviations, respectively. *B*, voltage and current traces for a typical pulse that activates membrane currents. Holding, test and repolarizing potentials were -90, 0 and -40 mV, respectively. Ringing shown in this example was not frequent, but if present it never lasted longer than four to five cycles.

duty cycle of 0·3. The combination of low-resistance patch pipettes and discontinuous voltage clamp for clamping fast sodium currents in BSNs has been reported elsewhere (Jones, 1987). Using this method, series resistance errors are negligible provided that electrode voltage settles at the end of each cycle. This was achieved by proper use of the stray capacitance neutralization (Finkel & Redman, 1984).

Critical damping was obtained by minimizing the width of capacity transients. Generally, capacity transients after voltage commands that did not evoke active membrane currents were largely completed within one cycle (i.e. 20–25 μs; see Fig. 1*A*). However, when membrane conductance had been increased (Fig. 1*B*), two kinds of error arose (Finkel & Redman, 1984; Jones, 1987). The first one was the low steady-state gain error, due to discharging of membrane capacitance during 70% of the cycle, and it was proportional to the amount of current. Using a typical value of 10 nA/mV for the transconductance loop gain gave errors of a very few millivolts. The other source of error was the presence of 'ripple'. It worked in the opposite direction and tended to cancel the error due to low steady-state gain. Although the voltage errors were expected to be small with appropriate settings, computer simulations were carried out in order to determine to what extent data obtained from experiments were distorted by the use of different single-electrode voltage-clamp techniques (F. Sala, in preparation). If simulated currents were analysed following the procedure described below, the parameters obtained were almost identical to those specified in the simulation.

Data acquisition and analysis

Current and membrane potential were first recorded on magnetic tape filtered at 20 kHz, then digitized at 40–80 kHz using ASYSTANT software (McMillan Software, Co.) with a DT2818 A–D interface (Data Translation) and stored on the hard disc of a PC/AT for subsequent analysis.

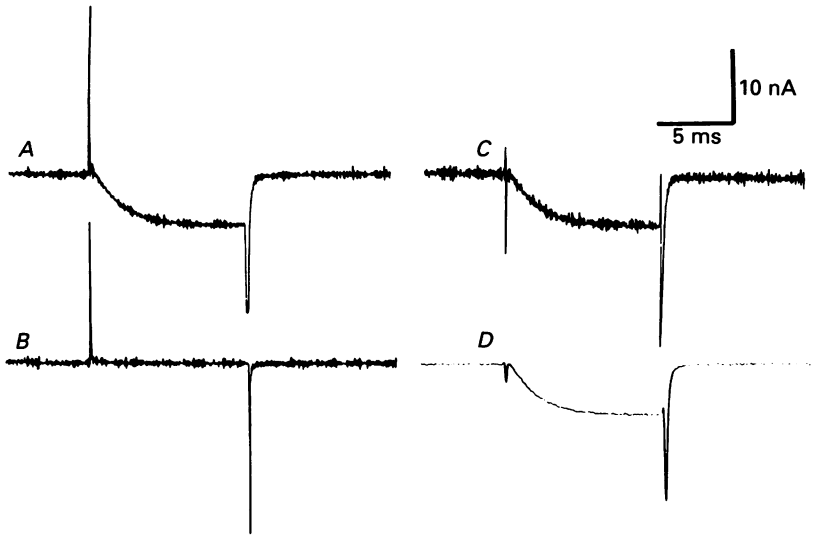

Fig. 2. Typical treatment of current records. *A*, inward current obtained at +10 mV from a holding potential of −90 mV. $[Ca^{2+}]_o = 4$ mM. This kind of raw trace was used for tail current analysis. *B*, same as in *A* but in the presence of 200 μM-Cd^{2+} which completely blocks the inward current. *C*, subtraction of *A* and *B* gives the net calcium current. *D*, same trace as in *C* after filtering with a cut-off frequency of 0·25 cycles/point. This kind of trace was used in the analysis of onset kinetics and peak current.

For tail current analysis neither linear leakage nor capacitive currents were subtracted from the recorded traces, and no filter was used. To evaluate the time course of ionic Ca^{2+} current activation, asymmetry currents presumably due to Ca^{2+} channel gating current (Adams & Gage, 1976; Kostyuk, Krishtal & Pidoplichko, 1981; Brown, Tsuda & Wilson, 1983) were eliminated by subtracting currents recorded in the presence of 200 μM-Cd^{2+}. After that, traces were digitally filtered with a cut-off frequency of 0·25 cycles per point. Figure 2 shows a typical treatment of a current trace. In all cases, data collected in the first 200 μs after a voltage step were discarded and not considered in the analysis.

All fits were done using the Gauss–Newton method of approximation. Data manipulation, analysis and plotting were done using ASYSTANT and other programs written in ASYST language (McMillan Software, Co.).

RESULTS

Isolation of Ca^{2+} currents

To study Ca^{2+} current kinetics it is necessary to eliminate other membrane currents that could distort the time course of the Ca^{2+} currents. Sodium currents were eliminated by replacing external sodium with sucrose. Potassium currents were blocked by the presence of Cs^+, TEA and 4-AP in the external solution and Cs^+ or TEA internally. The development of Ca^{2+}-activated currents was impaired by the inclusion of the calcium chelator BAPTA (5 mM). Under these experimental

conditions an inward current was activated by membrane depolarization above −40 mV. This inward current was identified as the Ca^{2+} current because the amplitude of the current increased with increases in $[Ca^{2+}]_o$ and Sr^{2+} and Ba^{2+} could carry this current as well (not shown). Furthermore, the inward current was blocked in the presence of the divalent cations Co^{2+} and Cd^{2+}, which block Ca^{2+} currents in other preparations (Hagiwara & Byerly, 1981).

Even under these conditions there was some evidence for the presence of small contaminating currents. Upon repolarization to −40 mV after a 10 ms depolarization, a slow tail current was observed which did not appear to be related to calcium channel closure (see below). Also, generally, the amplitudes of the tail currents grew and decayed in parallel with those of the inward current measured at the end of the depolarizing pulse (see Figs 3 and 5). Nevertheless, this was not always true. In some cells, inward currents evoked by long depolarizing pulses to positive potentials inactivated more than tail currents did, suggesting the development of a slowly activating outward current. Such a contaminating current has been reported in these cells to be associated with slowly decaying tails (Jones & Marks, 1989), and could be due to a Ca^{2+}-activated chloride current (Miledi & Parker, 1984) as suggested for cat sensory neurones (Taylor, 1988*a*).

Tail currents

Voltage-dependent Ca^{2+} currents that activated during membrane depolarization deactivated on repolarization. The increased driving force gave rise to tail currents that decayed in magnitude as Ca^{2+} channels shut. The magnitude of the tail current increased with increasing duration of the depolarizing pulse. This growth of tail currents paralleled the development of the inward current recorded during the pulse. Figure 3 illustrates this point by showing the very similar time course of both parameters. This close correspondence strongly suggests that tail currents were the result of the deactivation of the previously activated Ca^{2+} current.

In the cell of Fig. 3, tails at −30 mV decayed with a single-exponential time course (time constant, $\tau \approx 500$ μs). Nevertheless, the presence of a slower component with a time constant of 1–5 ms and with small amplitude (≈ 1/20–50th of the fast component amplitude) was not unusual and has also been found in this preparation by Jones & Marks (1989). Many cells showed such slow components in the tails (see Figs 4 and 5), but the following points argue against their significance as a component of the Ca^{2+} tail current. First, they were not present in every cell where calcium currents were recorded. Second, their amplitude and time constant were often dependent on the pulse duration rather than on the membrane potential (i.e. for pulses of 100 ms or longer some cells showed slow tail currents with time constants of tens of milliseconds; not shown). Third, their small amplitude after pulses of 10 ms makes it unlikely that they might reflect the existence of an additional closed state of the channel as has been suggested in other studies (Brown *et al.* 1983; Byerly, Chase & Stimers, 1984*a*; Taylor, 1988*a*). Hence, the slow component of the tail current is not considered further in the kinetic analysis.

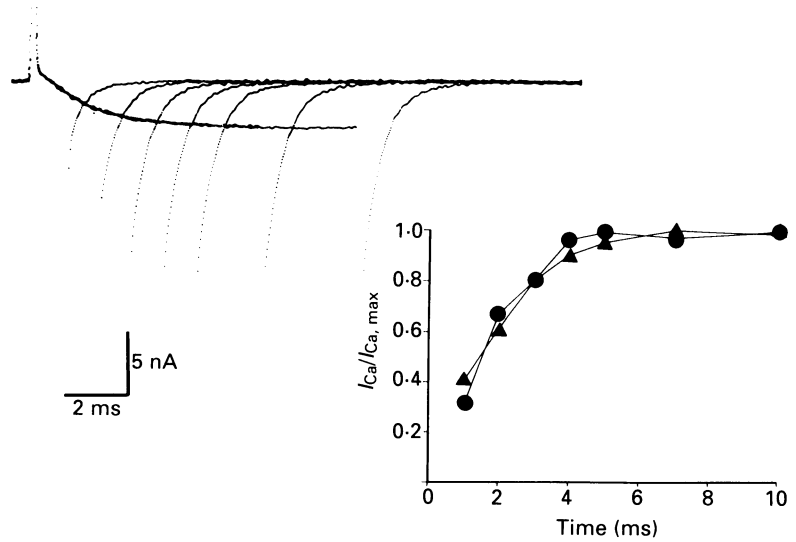

Fig. 3. Development of tail currents with pulse duration. *A*, seven records taken during pulses to +10 mV. Pulse durations were 1, 2, 3, 4, 5, 7 and 10 ms. Holding and repolarizing potentials were −80 and −30 mV, respectively. Records have been smoothed at 0·25 cycles/point. Eight points (200 μs) after the repolarizing step have been blanked. The graph shows normalized currents measured at the end of the pulses (▲), and by extrapolation of the tails to $t = 0$ (●).

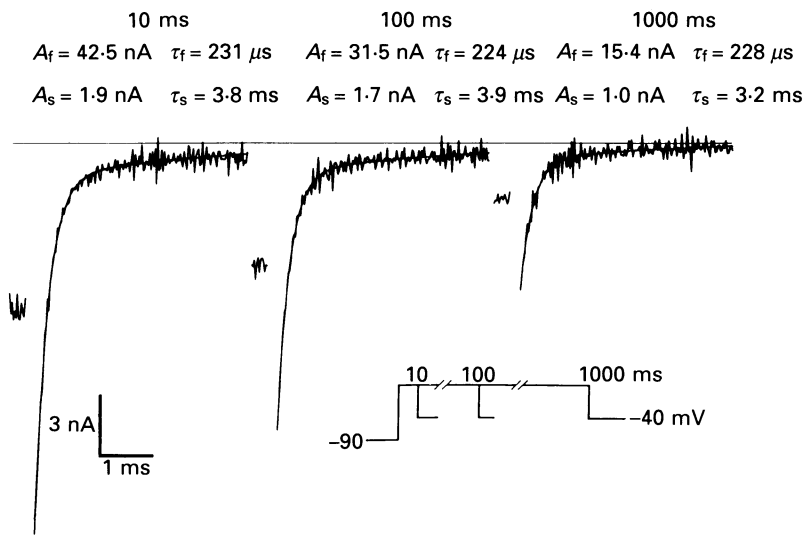

Fig. 4. Calcium tail currents after pulses of different duration (10, 100 and 1000 ms) to +10 mV from a holding potential of −90 mV. Inward currents at the end of the pulse were 8·6, 6·0 and 2·9 nA, respectively (small traces at the left of the tails). Smooth curves are the best fits to two exponentials. After the repolarizing step, 200 μs have been blanked. Amplitudes (A_f and A_s) are extrapolations to $t = 0$.

Different types of calcium channels?

Nowicky *et al.* (1985) first postulated the existence of multiple types of calcium channels in chick dorsal root ganglion (DRG) cells, namely T, N and L types, on the basis of whole-cell and single-channel recordings. The co-existence of the N and L

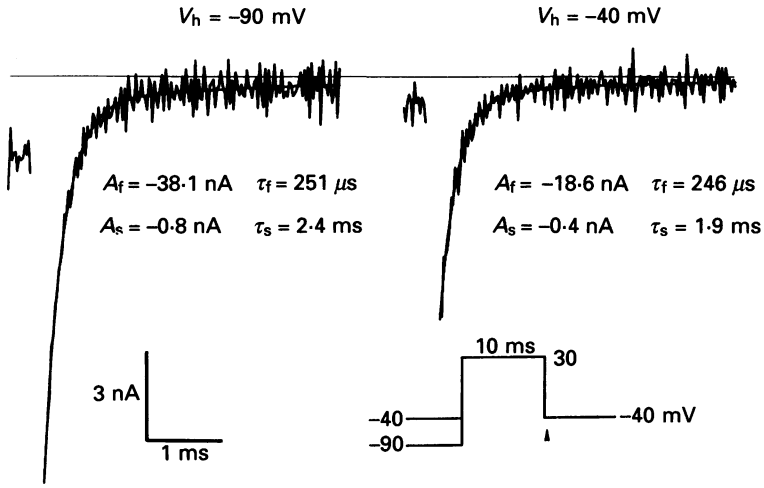

Fig. 5. Calcium tail currents after 10 ms pulses to +30 mV from different holding potentials (−90 and −40 mV). Inward currents at the end of the pulses were 2·3 and 1·0 nA, respectively (small traces at the left of the tails). Smooth curves are the best fits to two exponentials. After the repolarizing step, 200 μs have been blanked. Amplitudes are extrapolations to $t = 0$. All recordings were at least 3–5 min after any change of holding potential.

type of calcium channels has been reported in frog sympathetic ganglion cells (Lipscombe, Madison, Poenie, Reuter, Tsien & Tsien, 1988). In order to dissect kinetically these two components two different tests were employed.

(a) According to the N-channel hypothesis, N channels should inactivate during prolonged depolarization (Nowicky *et al.* 1985; Fox, Nowicky & Tsien, 1987). Depolarizing the membrane from a holding potential of −90 mV evoked a calcium current that decayed partially with time. The inactivating component has been claimed to be carried through N channels. If that is true and deactivation kinetics are different for the two components, tail kinetics would be expected to change as the contribution of N channels diminishes. Figure 4 shows that at the end of voltage pulses of increasing length, inward currents were progressively smaller and so were the amplitudes of the subsequent tail. However, despite inactivation of a putative N component, tail currents relaxed with the same time course after a pulse of 10 ms or after a pulse of 1000 ms where almost two-thirds of both current and tail had inactivated.

(b) Ca^{2+} currents evoked from more depolarized holding potentials were smaller and their rate of inactivation during long pulses was also slower than when evoked from −90 mV. This agrees with the disappearance of a presumably voltage-dependent inactivating component that could correspond to the N current. Thus, tail

currents after pulses evoked from −40 mV should be mostly carried through L channels, whereas those after pulses evoked from −90 mV should be carried through a mixture of L and N channels. Again, unless deactivation rates of both channels are identical, tail currents would decay with different time courses. Figure 5 shows that

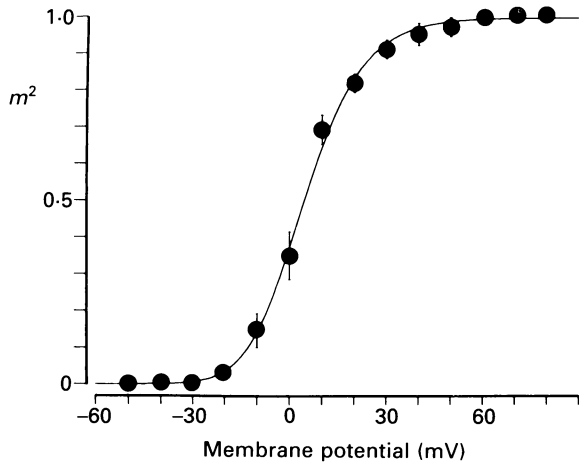

Fig. 6. Steady-state activation of the Ca^{2+} current derived from tail measurements. Tail current amplitudes were normalized to the tail amplitude after a pulse to +60 mV. Data represented as mean and standard error ($n = 7$). Continuous line is given by eqn (3) with the parameters of the text. Error bars are shown if bigger than symbols.

the tail evoked from −40 mV had roughly the same time constants as that from −90 mV (246 and 251 μs for the fast component, respectively). The similarity of time constants was found regardless of the test potential.

Thus, Ca^{2+} current activation kinetics in these neurones can be studied as if there was only a single population of Ca^{2+} channels. This assumption is made throughout the remainder of the results. In addition to this tentative conclusion, the similarity of the tail time constants in spite of their magnitude provides additional support for the idea that errors due to low amplifier gain should be small.

Steady-state activation

According to the scheme used to fit Na^+ and K^+ currents in squid axon (Hodgkin & Huxley, 1952), calcium current, I_{Ca}, may be described by:

$$I_{Ca}(V,t) = I_{Ca,max}(V)\, m^x(V,t), \tag{1}$$

where $I_{Ca,max}(V)$ is the maximal calcium current as a function of voltage, x is an integer and m is a variable that ranges from 0 to 1. The term $m^x(V,t)$ reflects the fraction of Ca^{2+} conductance as a function of voltage and time.

The differential equation describing the change of m is given by:

$$dm(V,t)/dt = \alpha_m(V) - [\alpha_m(V) + \beta_m(V)]\, m, \tag{2}$$

where α_m and β_m are the first-order rate constants governing the channel opening and closing, respectively.

In the steady state, the fraction of Ca^{2+} permeability (m^x) or, in other words, the

probability that the channel is open as a function of voltage, can be estimated by measuring the amplitude of the tail currents upon repolarization to −40 mV after 10 ms activating pulses. This short time allows the current to fully activate (more than 99% even with the largest activation time constant) with minimal

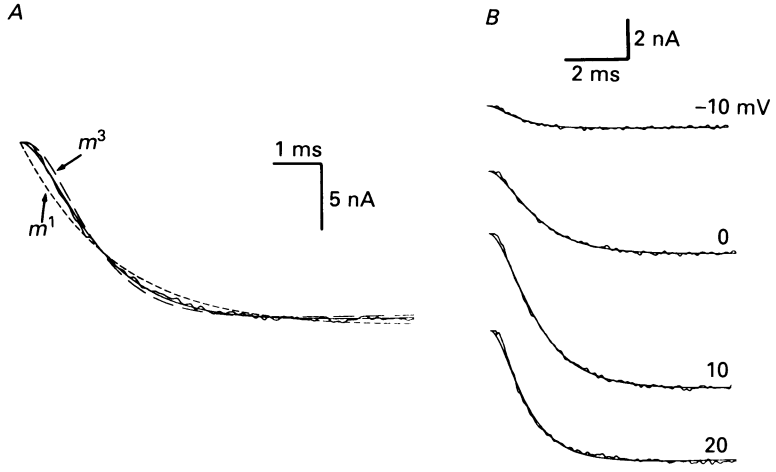

Fig. 7. *A*, current record for a pulse to +10 mV from −90 mV with best fits of m^1 form (fine dashed line), m^2 form (continuous line) and m^3 form (coarse dashed line). *B*, Ca^{2+} current records obtained at the potentials indicated. The smooth curve drawn through each trace is the m^2 expression fitted to the data. Time constants (τ_m) were 0·718, 1·060, 1·057 and 0·787 ms, from top to bottom.

contamination by other currents or inactivation which both develop with a time course of hundreds of milliseconds. The magnitude but not the time course of the tail was found to depend on the pulse potential.

The normalized, averaged results from nine cells are shown in Fig. 6. This activation curve has a sigmoidal form and was fitted by a Boltzmann expression:

$$m^x(V) = 1/[1+\exp((V_{\frac{1}{2}}-V)/V_k)]^x, \quad (3)$$

where the mid-point voltage ($V_{\frac{1}{2}}$) is −4·7 mV, the steepness factor (V_k) is 10·5 mV, and $x = 2$.

Turn-on kinetics

The solution of eqn (2) after a voltage step is:

$$m^x(V,t) = [m_\infty-(m_\infty-m_o)\exp(-t/\tau_m(V))]^x, \quad (4)$$

where m_∞ and m_o are the final and initial value of m, τ_m is the membrane time constant which equals $1/[\alpha_m(V)+\beta_m(V)]$, and x is the integer that best fits the time course of activation.

Figure 7 shows that at the onset of a depolarizing pulse the Ca^{2+} current activated sigmoidally with a variable delay. Contributions from gating currents that dominate the earlier part of activation were minimized by subtracting corresponding responses in the presence of 200 μM-Cd^{2+}. Similar attempts were made in the presence of 5 mM-

Co^{2+} but, unlike Brown *et al.* (1983), the subtraction procedure always gave a considerable outward current at the onset. It seems likely that that was due to differential surface charge screening effect.

The expression that best fits the data has the m^2 form as illustrated in Fig. 7*A* where the disagreement with the m^1 or m^3 fits is also shown. Current at time zero was always taken as zero. However, in three out of nine cells when holding at −90 mV (but not at −40 mV), the fit to the m^3 form was as good or slightly better than that to the m^2 form, indicating some evidence in favour of a Cole–Moore-type shift observed by these authors for the squid axon potassium current, where higher values of x were needed to describe its activation as the holding potential was made more negative (Cole & Moore, 1960).

Figure 7*B* shows that the m^2 form fitted well the activation time course of Ca^{2+} currents evoked at different test potentials. The time constants (τ_m) obtained by this method were dependent on the test potential and had a maximum around 0 mV (Fig. 8), but they were insensitive to the holding potential.

Turn-off kinetics

Tail current analysis was done without correction for gating currents since they are expected to contribute little to the total current and because of the voltage-dependent block of Cd^{2+} (Taylor, 1988*b*). Like the time course of activation, deactivation of Ca^{2+} current was also strongly dependent upon the membrane potential at which the tail current was measured. At more negative potentials tail currents decayed more rapidly.

According to m^2 kinetics, eqn (4) implies that tail currents should decay with two exponential time constants, one being half of the other. For potentials where the steady-state value of m is zero, the time course of the tail should be single exponential with a time constant (τ_f) of 0·5 τ_m. At more positive potentials tails could also be fitted by a single exponential using an approximate expression relating τ_f to τ_m, which was derived from eqn (4) by Hagiwara & Ohmori (1982): $\tau_f = \tau_m(m_\infty + m_o)/2\, m_o$. Using this expression the values of τ_m can be derived from those of τ_f.

Figure 8*A* shows that values of τ_m derived from activation and deactivation measurements have a bell-shaped dependence on membrane potential expected from a voltage-gated channel.

From eqns (2) and (4), time constants α_m and β_m are related to m_∞ and τ_m by the expressions $m_\infty = \alpha_m/(\alpha_m + \beta_m)$ and $\tau_m = 1/(\alpha_m + \beta_m)$. Since values of m_∞ and τ_m can be measured at different potentials, the corresponding values of the rate constants can be easily calculated, Figure 8*B* shows such values over a wide range of membrane potential. Continuous lines are fits with the following expressions:

$$\alpha_m(V) = 0{\cdot}058\ (11{\cdot}3 - V)/[\exp((11{\cdot}3 - V)/13{\cdot}7) - 1], \quad (5)$$

$$\beta_m(V) = 0{\cdot}085\ (V + 15{\cdot}4)/[\exp((V + 15{\cdot}4)/9{\cdot}9) - 1], \quad (6)$$

where α_m and β_m are given in ms^{-1} and V is the membrane potential in millivolts.

These relationships are less steep at extreme potentials than those predicted by the rate theory model (Stevens, 1978) but this could reflect limitations in the voltage-clamp performance (see Discussion).

Open-channel I–V relationship

If all the Ca^{2+} channels are opened by giving a pulse to +60 mV and then the membrane is repolarized to various potentials, the amplitude of the subsequent tail currents extrapolated to time zero should give the maximal calcium current at these

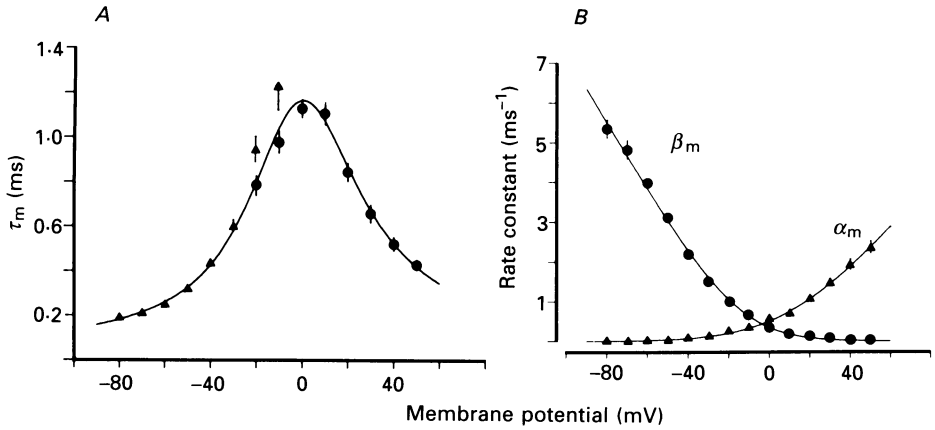

Fig. 8. *A*, time constants of activation for an m^2 model derived from turn-on (●) and turn-off (▲) Ca^{2+} currents. Time constants from tails were derived from a single-exponential fit to tail currents at these potentials and corrected as mentioned in the text. The continuous line is given by $\tau_m(V) = 1/[\alpha_m(V)+\beta_m(V)]$ where α_m and β_m are given by eqns (5) and (6). *B*, rate constants of activation for an m^2 model calculated as explained in the text. Continuous lines are given by eqns (5) and (6). Data represented as mean and standard error ($n = 10$). Error bars are shown if bigger than symbols.

potentials ($I_{Ca,max}$) and the plot of those currents against the potentials at which they were measured would give the open-channel *I–V* relationship. Figure 9*A* illustrates that as expected for a highly asymmetric distribution of calcium ions, the relation showed a strong rectification at positive potentials.

Values above −30 mV could be matched (dashed line in Fig. 9*A*) by the constant-field equation (Goldman, 1943; Hodgkin & Katz, 1949) but amplitudes at more negative potentials were bigger than predicted by theory. In addition, amplitudes of tails at potentials negative to −80 mV seemed to saturate, but this could not be established because of their fast time course. For $[Ca^{2+}]_o = 4$ mM, the modified form shown below fitted better the data at potentials positive to −90 mV:

$$I(V) = PV(D-\exp(-V/C))/[1-\exp(V/C)], \quad (7)$$

where $P = -0{\cdot}267$ nA/mV, $D = 0{\cdot}2$ and $C = 45$ mV. This form includes a term, D, in order to account for outward currents at positive potentials (see Discussion).

Reconstructed I–V relationship

According to eqn (1), the product of the functions described in eqns (3) and (7) must allow calculation of the steady-state calcium current at any voltage. The *I–V* relationship is taken as the peak current after 10 ms depolarizing pulses of different

size. The average steady-state current of nine cells is represented in Fig. 9*B*. The continuous line represents theoretical values using eqns (3) and (7). The dashed line was constructed using a constant-field equation of the form shown in the figure legend. Since the constant-field equation fitted well the instantaneous *I–V*

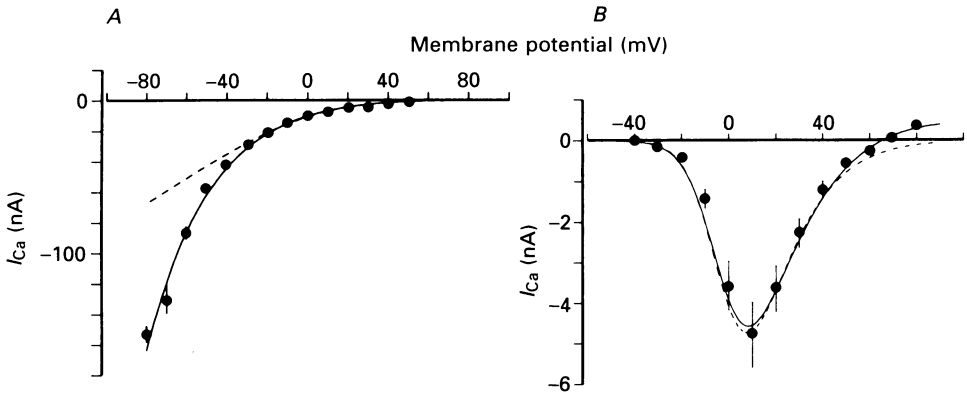

Fig. 9. *A*, instantaneous *I–V* relationship for $[Ca^{2+}]_o = 4$ mM. Continuous curve is given by eqn (7). Dashed line is given by the constant-field expression $I(V) = PV\exp(-V/12{\cdot}5)/[1-\exp(-V/12{\cdot}5)]$, where $P = -0{\cdot}842$ nA/mV. *B*, peak *I–V* and constructed peak *I–V* relationships. These were obtained by multiplying eqn (3) and the functions describing the instantaneous *I/V* relationship (continuous line took eqn (7) and dashed line took the constant-field expression of *A*). Data are mean and standard error ($n = 9$). Error bars are shown if bigger than symbols.

relationship above −30 mV, the experimental peak *I–V* relationship was fitted reasonably, too.

DISCUSSION

Kinetic properties of the macroscopic Ca^{2+} current have been analysed in a number of tissues from different animals (for review, see Hagiwara & Byerly, 1981). In BSNs, previous analyses have been performed using the two-electrode voltage-clamp technique (Adams, 1980). The present study differs from that of Adams (1980) in the use of dissociated cells that allows a much better space-clamp condition, and also in the use of the single-electrode patch-clamp technique. Recently a similar analysis with continuous voltage clamp has been reported (Jones & Marks, 1989). The combination of discontinuous single-electrode voltage-clamp switching at high frequencies and a low-resistance patch pipette provides a suitable method to clamp fast Ca^{2+} currents, and therefore allows the study of their activation kinetics. Computer simulations showed that distortions due to the discontinuous clamp are small for a typical BSN Ca^{2+} current (F. Sala, in preparation).

How many types of calcium channels?

Hagiwara, Ozawa & Sand (1975) first reported the co-existence of two types of Ca^{2+} channels in egg cells. These two types correspond to LVA (low voltage activated) or T type and HVA (high voltage activated) or L type according to the

current nomenclature. Since then much effort has been devoted to isolating the different types in other preparations. The co-existence of these two types has been extensively demonstrated in a number of tissues (for review see Tsien *et al.* 1988).

BSNs lack the type of Ca^{2+} channel called LVA or T. The current carried by these channels can be easily separated from other types of Ca^{2+} channels since it activates around -50 mV producing a marked shoulder in the peak I–V curve, and it is fully inactivated at holding potentials positive to -60 mV. There is no evidence for such a current in these neurones. In addition, a third type, the N channel, has been described with intermediate properties between the two previously established types (Nowicky *et al.* 1985). Its identification is based on macroscopic, microscopic and pharmacological criteria. Such channels and currents with properties compatible with the N type have been found in frog sympathetic neurones (Lipscombe *et al.* 1988). None the less the characterization of the N current is not as complete as could be desired (Tsien *et al.* 1988).

Since the aim of the present work was to analyse the activation kinetics of Ca^{2+} currents in BSNs, the first step to be taken was to find out how many components of the Ca^{2+} current could be separated in terms of activation kinetics behaviour. It has been shown that fast tail currents reflecting the closing of Ca^{2+} channels relaxed with a single-exponential time course. This suggests that the channels underlying the fast tail current belong to a kinetically homogeneous type, but does not provide direct evidence of that. On the other hand, there remains the existence of slow tails. It has been recently reported that N current deactivates with a slower time course than L current in mice sensory neurones (Kostyuk & Shirokov, 1989). Therefore, it could be argued that the slow tail found in many cells could represent the closing of a different type of Ca^{2+} channel. This hypothesis has been discarded in the present study by the following arguments: (1) the amplitude of the slow tail was very small after short pulses (10 ms) and did not consistently parallel the amplitude of the current after longer pulses; e.g. in many cases the current inactivated whereas the amplitude of the slow tail continued growing. (2) Its time course never depended on the potential but often on the pre-pulse duration. This is unlikely for N channels if they are purely voltage gated. (3) The slow tail remained under experimental conditions that should inactivate the N component according to Nowicky *et al.* (1985). In cells that had the slow tail, holding the membrane potential at more positive values did not change the slow tail amplitude relative to that of the fast tail, suggesting that the former is not selectively supressed as would be expected.

However, it still remains possible that the fast tail is the sum of two deactivation processes which could not be resolved properly. Thus additional tests were made in order to explore the above possibility. It was found that fast tails had the same decay kinetics after currents evoked from different holding potentials (Fig. 5) or after pulses of variable duration (Fig. 4). Although both tests provide different degrees of inactivation of the putative N component, the first protocol at steady state and the second one dynamically, tail kinetics did not change. Moreover, turn-on kinetics were also found to be independent of the holding potential. Taken together these facts indicate that activation of Ca^{2+} currents in BSNs can be treated as if there were only a single population of Ca^{2+} channels. Similar results have been considered as evidence for the existence of a single population of HVA channels in DRG neurones,

corresponding to L type (Swandulla & Armstrong, 1988), but with the results shown here it is not possible to discard the possibility that Ca^{2+} current of BSNs is carried through a mixture of N and L channels, or even through mostly N channels. In fact, Jones & Marks (1989) tentatively concluded that N-type Ca^{2+} current predominates in these cells with a minor contribution of L-type current, in agreement with other studies done in mammalian neurones (Plummer, Logothetis & Hess, 1989). Neither single-channel analysis nor pharmacological tests have been carried out in the present work to resolve this issue.

Activation of the Ca^{2+} current

This analysis was done in a time domain (up to 10 ms) where inactivation of calcium current is negligible and where important physiological events (i.e. action potentials) take place. The voltage dependence of the fraction of Ca^{2+} permeability activated was determined by the size of tail currents (Fig. 6). Calcium permeability (m^2) is half-activated between 0 and +5 mV, close to the voltage where maximum steady-state current is recorded and where the kinetics are slowest (see Figs 8*A* and 9*B*), as has been found in other preparations (Fenwick, Marty & Neher, 1982; Hagiwara & Ohmori, 1982; Brown *et al.* 1983). In BSNs, Jones & Marks (1989) have reported a half-activation voltage of −5 mV, the other parameters also being shifted to the left by roughly 10 mV with respect to the present study. This discrepancy could be due to either the different extracellular concentration of calcium used, or the correction of offset potentials, or both. The activation curve was fitted by a Boltzmann distribution raised to the second power. This is expected from a Hodgkin–Huxley model where the state of the channel is controlled by the movement of two independent and equally charged gating particles in the electrical field with a mid-point voltage of −4·7 mV and a steepness factor of 10·5 mV for each particle.

It can be seen in Fig. 6 that tail amplitudes do not completely saturate at positive potentials as predicted by the simple Hodgkin–Huxley model but continue increasing slightly. This may be due to a small degree of facilitation of the current by large depolarizing steps as described by others (Hoshi, Rothlein & Smith, 1984; Jones & Marks, 1989). Also it may be interpreted in terms of a more complex model with non-equally charged gating particles (Taylor, 1988*a*).

Activation of Ca^{2+} currents in other preparations such as snail neurones (Kostyuk *et al.* 1981; Byerly & Hagiwara, 1982; Brown *et al.* 1983; Byerly *et al.* 1984*a*), pituitary cells (Hagiwara & Ohmori, 1982), rat sympathetic neurones (Belluzzi & Sacchi, 1989) and hippocampal neurones (Kay & Wong, 1987), has been shown to follow m^2 kinetics. In contrast, chromaffin cell Ca^{2+} currents have been fitted with a two-exponential form (Fenwick *et al.* 1982), cat sensory neurones Ca^{2+} currents were best fitted with a three-exponential form (Taylor, 1988*a*) and a m^5 form was required to fit Ca^{2+} currents in squid giant synapse (Llinás, Steinberg & Walton, 1981).

Previous studies in BSNs have shown that the m^1 form describes most of the Ca^{2+} current data but does not account for the delay observed at the onset of the currents (Adams, 1980; Jones & Marks, 1989). In the present study it has been found that, after proper elimination of gating currents, the time course of the onset follows quite well m^2 kinetics at all test potentials. Also, most data obtained from tail currents

measurements are consistent with m^2 kinetics. This implies a linear sequential model with two closed states and one open state.

Two tests can be made to check m^2 kinetics. Currents evoked from depolarized potentials should activate with roughly m^1 kinetics (Kostyuk *et al.* 1981; Byerly *et al.* 1984*a*). This is so because a large fraction of Ca^{2+} channels is in a state that only needs to make one transition to reach the open state. Such a test was succesfully met (not shown). The second test is to compare membrane time constants (τ_m) derived from activating and deactivating currents in the voltage region where both can be accurately measured. With this method time constants derived from tail currents were always larger than those derived from turn-on measurements (see Fig. 8*A*). Several factors could account for this disagreement: (1) because of the bigger currents, voltage-clamp conditions are always poorer during the tails than during the pulses. Computer simulations indicated that time constants of the tails are 10–30% larger than those measured during the onset at the same potential (F. Sala, in preparation); (2) the expression used to approximate τ_m from τ_f (Hagiwara & Ohmori, 1982) always gives overestimates of τ_m; (3) the slowly decaying but large tail currents occurring at these potentials could activate a Ca^{2+}-dependent chloride inward current which would further slow the time course of the tails.

Alternatively, the discrepancy could be explained by a model with four states as suggested by Hagiwara & Ohmori (1983) which, with a third closed state connected to the open state with voltage-independent rates, predicts the turn-on to be faster than the turn-off.

Values of α_m and β_m for the m^2 model were calculated from experimental values of m_∞ and τ_m. At negative potentials the value of β_m is roughly $1/(2\,\tau_f)$. Since values of τ_f can be overestimated by clamp errors, β_m can be underestimated at these potentials, thus increasing less than expected for a pure Boltzmann distribution. A four-state model like that mentioned above could also account for the apparent deviation from the theory. However, the experimental conditions did not allow accurate discrimination between models. Thus, the simplest m^2 model was favoured in this study. According to it the predicted mean open time of the Ca^{2+} channel at 0 mV would be 1·4 ms, in agreement with that found for Ca^{2+} channels in chromaffin cells which was around 1 ms (Fenwick *et al.* 1982).

The open-channel *I–V* relationship shows the typical rectification at positive potentials for low internal concentration of the permeant cation and could be fitted more or less well by a variety of expressions. The constant-field equation for $[Ca^{2+}]_i = 0$ can fit well the relation for potentials above -30 mV. Nevertheless the equation predicts smaller amplitudes below that potential and this could not be accounted for by voltage-clamp errors which would cause the calculated amplitudes to be smaller than the real ones. A modified form of the constant-field equation as used by Brown *et al.* (1983) can describe the data but it is necessary to incorporate a correction factor for positive potentials. Other authors have reported the observed currents at positive potentials to be carried not only by Ca^{2+} but also by Cs^+ passing through Ca^{2+} channels (Fenwick *et al.* 1982) or by H^+ through distinct channels (Byerly, Meech & Moody, 1984*b*). The term *D* in eqn (7) would account for all these contaminating outward currents. According to that, the apparent reversal potential would be around +70 mV, in agreement with experimental observations. The accuracy with

which the open-channel I–V function describes the results at positive potentials determines the accuracy with which the reconstructed peak I–V relation matches the observed currents.

Another way to describe the open-channel I–V relationship is by means of appropriate parameters in a symmetric two-site three-barrier rate theory model (not shown) as previously proposed (Almers & McCleskey, 1984; Hess & Tsien, 1984; Taylor, 1988*b*). Such a model would have the advantage of explaining several features of the Ca^{2+} currents that seem to deviate from the independence principle. Among them there is the anomalous mole-fraction effect which is evident in mixtures of calcium and barium ions (Almers & McCleskey, 1984; Hess & Tsien, 1984; Byerly, Chase & Stimers, 1985; Friel & Tsien, 1989) and which has been also found in BSNs (F. Sala, unpublished results). However, with the experiments done in this study it seems preferable not to draw conclusions about selectivity and permeation mechanisms which would need single-channel data.

A mean elementary current of around 0·1 pA at −12 mV has been extracted from noise analysis of Ca^{2+} current recordings in 5 mM-Ca^{2+} in bovine chromaffin cells (Fenwick *et al.* 1982). Assuming this amplitude and using the data of Fig. 9*A*, the density of Ca^{2+} channels in BSN somata could be estimated at around 30 channels/μm^2. Although this is a higher density than that found in bovine chromaffin cells (Fenwick *et al.* 1982), it is similar to that found in snail neurones (Krishtal, Pidoplichko & Shakhovalov, 1981) and rat sympathetic neurones (Belluzzi & Sacchi, 1989) where it has been reported to be 30–60/μm^2.

Conclusion

From the data presented here it can be concluded that BSN Ca^{2+} currents can be treated as carried through a single population of channels insofar as activation kinetics are concerned. As in other preparations (Swandulla & Armstrong, 1988), dissection of N and L components in macroscopic Ca^{2+} currents was not possible using tail current analysis. None the less, the results do not rule out that this could be achieved by using pharmacological tests. Most of the whole-cell Ca^{2+} current activation kinetics can be accounted for by a simple Hodkgin–Huxley model with a m^2 form. This quantitative description can be useful in modelling the electrical behaviour of BSNs if incorporated in a more complete model of BSNs, which would include intracellular calcium diffusion and several potassium currents dependent on intracellular calcium concentration (see Yamada, Koch & Adams, 1989, and Sala & Hernández-Cruz, 1990).

I wish to thank Professor Paul R. Adams for providing the facilities of his laboratory and for helpful discussion. I also thank Professor Erwin Neher and Dr Neil V. Marrion for comments on the manuscript, Mr B. Burbach for tissue culture and photography, and A. Villarroel for helping with illustrations. I was supported by Fundación Juan March (Spain).

REFERENCES

ADAMS, D. J. & GAGE, P. W. (1976). Gating currents associated with sodium and calcium currents in an *Aplysia* neuron. *Science* **192**, 783–784.

ADAMS, P. R. (1980). The calcium current of a vertebrate neuron. In *Physiology of Excitable Membranes*, ed. SALANKI, J., pp. 135–138. Akademiai Kiado, Budapest.

ALMERS, W. & MCCLESKEY, E. W. (1984). Non-selective conductance in calcium channels of frog muscle: calcium selectivity in a single-file pore. *Journal of Physiology* **353**, 585–608.

BELLUZZI, O. & SACCHI, O. (1989). Calcium currents in the normal adult rat sympathetic neurone. *Journal of Physiology* **412**, 493–512.

BROWN, A. M., TSUDA, Y. & WILSON, D. L. (1983). A description of activation and conduction in calcium channels based on tail and turn-on current measurements in the snail. *Journal of Physiology* **344**, 549–583.

BYERLY, L., CHASE, P. B. & STIMERS, J. R. (1984*a*). Calcium current activation kinetics in neurones of the snail *Lymnaea stagnalis*. *Journal of Physiology* **348**, 187–207.

BYERLY, L., CHASE, P. B. & STIMERS, J. R. (1985). Permeation and interaction of divalent cations in calcium channels of snail neurons. *Journal of General Physiology* **85**, 491–518.

BYERLY, L. & HAGIWARA, S. (1982). Calcium currents in internally perfused nerve cell bodies of *Limnea stagnalis*. *Journal of Physiology* **322**, 503–528.

BYERLY, L., MEECH, R. & MOODY, W. JR (1984*b*). Rapidly activating hydrogen ion currents in perfused neurones of the snail, *Lymnaea stagnalis*. *Journal of Physiology* **351**, 199–216.

COLE, K. S. & MOORE, J. W. (1960). Potassium ion current in the squid giant axon: dynamic characteristics. *Biophysical Journal* **1**, 1–14.

FENWICK, E. M., MARTY, A. & NEHER, E. (1982). Sodium and calcium channels in bovine chromaffin cells. *Journal of Physiology* **331**, 599–635.

FINKEL, A. S. & REDMAN, S. (1984). Theory and operation of a single microelectrode voltage clamp. *Journal of Neuroscience Methods* **11**, 101–127.

FOX, A. P., NOWICKY, M. C. & TSIEN, R. W. (1987). Kinetic and pharmacological properties distinguishing three types of calcium currents in chick sensory neurones. *Journal of Physiology* **394**, 149–172.

FRIEL, D. D. & TSIEN, R. W. (1989). Voltage-gated calcium channels. Direct observation of the anomalous mole fraction effect at the single channel level. *Proceedings of the National Academy of Sciences of the USA* **86**, 5207–5211.

GOLDMAN, D. E. (1943). Potential, impedance, and rectification in membranes. *Journal of General Physiology* **27**, 37–60.

HAGIWARA, S. & BYERLY, L. (1981). Calcium channel. *Annual Review of Neuroscience* **4**, 69–125.

HAGIWARA, S. & OHMORI, H. (1982). Studies of calcium channels in rat clonal pituitary cells with patch electrode voltage clamp. *Journal of Physiology* **331**, 231–252.

HAGIWARA, S. & OHMORI, H. (1983). Studies of single calcium channel currents in rat clonal pituitary cells. *Journal of Physiology* **336**, 649–661.

HAGIWARA, S., OZAWA, S. & SAND, O. (1975). Voltage-clamp analysis of two inward current mechanisms in the egg cell membrane of a starfish. *Journal of General Physiology* **65**, 617–644.

HAMILL, O. P., MARTY, A., NEHER, E., SAKMANN, B. & SIGWORTH, F. J. (1981). Improved patch-clamp techniques for high-resolution current recording from cells and cell-free membrane patches. *Pflügers Archiv* **391**, 85–100.

HESS, P. & TSIEN, R. W. (1984). Mechanism of ion permeation through calcium channels. *Nature* **309**, 453–456.

HODGKIN, A. L. & HUXLEY, A. F. (1952). A quantitative description of membrane current and its application to conduction and excitation in nerve. *Journal of Physiology* **117**, 500–544.

HODGKIN, A. L. & KATZ, B. (1949). The effect of sodium ions on the electrical activity of the giant axon of the squid. *Journal of Physiology* **108**, 37–77.

HOSHI, T., ROTHLEIN, J. & SMITH, S. J. (1984). Facilitation of Ca^{2+} channel currents in bovine chromaffin cells. *Proceedings of the National Academy of Sciences of the USA* **81**, 5871–5875.

JONES, S. W. (1987). Sodium currents in dissociated bull-frog sympathetic neurones. *Journal of Physiology* **389**, 605–627.

JONES, S. W. & MARKS, T. N. (1989). Calcium currents in bullfrog sympathetic neurons. I. Activation kinetics and pharmacology. *Journal of General Physiology* **94**, 151–167.

KAY, A. B. & WONG, R. K. S. (1987). Calcium current activation kinetics in isolated pyramidal neurones of the CA1 region of the mature guinea-pig hippocampus. *Journal of Physiology* **392**, 603–616.

KOSTYUK, P. G., KRISHTAL, O. A. & PIDOPLICHKO, V. I. (1981). Calcium inward current and related charge movements in the membrane of snail neurones. *Journal of Physiology* **310**, 403–421.

KOSTYUK, P. G. & SHIROKOV, R. E. (1989). Deactivation kinetics of different components of calcium inward current in the membrane of mice sensory neurones. *Journal of Physiology* **409**, 343–355.

KRISHTAL, O. A., PIDOPLICHKO, V. I. & SHAKHOVALOV, Y. A. (1981). Conductance of the calcium channel in the membrane of snail neurones. *Journal of Physiology* **310**, 423–434.

KUFFLER, S. W. & SEJNOWSKI, T. J. (1983). Peptidergic and muscarinic excitation at amphibian sympathetic synapses. *Journal of Physiology* **341**, 257–278.

LIPSCOMBE, D., MADISON, D. V., POENIE, M., REUTER, H., TSIEN, R. Y. & TSIEN, R. W. (1988). Spatial distribution of calcium channels and cytosolic calcium transients in growth cones and cell bodies of sympathetic neurons. *Proceedings of the National Academy of Sciences of the USA* **85**, 2398–2402.

LLINÁS, R., STEINBERG, I. Z. & WALTON, K. (1981). Presynaptic calcium currents in squid giant synapse. *Biophysical Journal* **33**, 289–322.

MARTY, A. & NEHER, E. (1983). Tight-seal whole-cell recording. In *Single-Channel Recording*, ed. SAKMANN, B. & NEHER, E., pp. 107–122. Plenum Press, New York.

MATTESON, D. R. & ARMSTRONG, C. M. (1986). Properties of two types of calcium channels in clonal pituitary cells. *Journal of General Physiology* **87**, 161–182.

MILEDI, R. & PARKER, I. (1984). Chloride current induced by injection of Ca into *Xenopus* oocytes. *Journal of Physiology* **357**, 173–188.

NOWICKY, M. C., FOX, A. P. & TSIEN, R. W. (1985). Three types of neuronal calcium channel with different calcium agonist sensitivity. *Nature* **316**, 440–443.

PLUMMER, M. R., LOGOTHETIS, D. E. & HESS, P. (1989). Elementary properties and pharmacological sensitivities of calcium channels in mammalian peripheral neurons. *Neuron* **2**, 1453–1463.

SALA, F. & ADAMS, P. R. (1989). Calcium currents activation kinetics in dissociated bullfrog sympathetic neurons. *Biophysical Journal* **55**, 300a.

SALA, F. & HERNÁNDEZ-CRUZ, A. (1990). Calcium diffusion modeling in a spherical neuron. Significance of buffering properties. *Biophysical Journal* **57**, 313–324.

STEVENS, C. F. (1978). Interactions between intrinsic membrane protein and electric field. *Biophysical Journal* **22**, 295–306.

SWANDULLA, D. & ARMSTRONG, C. M. (1988). Fast-deactivating calcium channels in chick sensory neurons. *Journal of General Physiology* **92**, 197–218.

TAYLOR, W. R. (1988*a*). Two-suction-electrode voltage-clamp analysis of the sustained calcium current in cat sensory neurones. *Journal of Physiology* **407**, 405–432.

TAYLOR, W. R. (1988*b*). Permeation of barium and cadmium through slowly inactivating calcium channels in cat sensory neurones. *Journal of Physiology* **407**, 433–452.

TSIEN, R. W., LIPSCOMBE, D., MADISON, D. V., BLEY, K. R. & FOX, A. P. (1988). Multiple types of neuronal calcium channels and their selective modulation. *Trends in Neurosciences* **11**, 431–438.

YAMADA, W. M., KOCH, C. & ADAMS, P. R. (1989). Multiple channels and calcium dynamics. In *Methods in Neuronal Modeling: From Synapses to Networks*, ed. KOCH, C. & SEGEV, I., pp. 97–133. MIT Press, Cambridge, MA, USA.